Macroscopic quantum effects in magnetic materials

Author: Ferran Aliagas Puigdomènech*
Dept. Física de la Matèria Condensada, Univ. de Barcelona, Av. Diagonal 647, 08028 Barcelona, Spain.

Advisor: Dr. Òscar Iglesias Clotas

Abstract: In this work, we present a theoretical study of Macroscopic Quantum Tunneling (MQT) for magnetic systems. To gain insights into its properties, Spin-coherent-state Feynman path integrals are used to calculate the tunneling transition rate, Γ, for single-domain ferromagnetic nanoparticles. We also compute the critical temperature T_c, which serves as the threshold between the quantum and thermal regime and we finally discuss experimental approaches that can provide empirical evidence of MQT in magnetic particles.

I. INTRODUCTION

Quantum mechanics is a field of physics well known for its unique and novel phenomena, however, due to its difficulty, these are commonly observed in the microscopic world and not at macroscopic scales. In this work, quantum tunneling, (one of most fascinating phenomena of quantum mechanics [1]) will be studied in the macroscopic regime [2].

The typical systems in which QT effects are observed (e.g. finite single well or double well potentials) are characterized by a probability transition rate (Γ) that depends exponentially on the quantity $-\mathcal{S}/\hbar$, being $\mathcal{S}$ the action [3]. For a heavy macroscopic particle: $\mathcal{S} \gg \hbar$, and, as a result, Γ is exponentially suppressed due to its high mass.

Therefore, different type of systems should be studied that present a greater probability of manifesting MQT. Magnetic systems are a great candidate for this purpose, some examples are QT of domain walls [4], QT of molecular magnets [5], or the object of this work: the study of MQT in single-domain uniaxial ferromagnetic nanoparticles (NP) [2, 6]. These particles can manifest MQT when the total magnetic moment ($\mathbf{M}$) rotates between the two stable states, overcoming the magnetic anisotropy energy barrier [7], without having enough thermal energy to do so. It is also referred as 'Spin Quantum Tunneling' (SQT), and the action in this case depends on the moment of inertia associated to the rotation of $\mathbf{M}$ and not explicitly on the mass of the particle [3]. To characterize SQT, the tunneling rate Γ at $T = 0$ K will be computed in the presence of an applied external magnetic field ($\mathbf{H}$) pointing perpendicular to the easy-axis. The Stoner-Wohlfarth model [8] and Feynman path integral formulation of quantum mechanics [9] will be used for this purpose. The calculations are based on the concept of instanton trajectories, which are classical solutions of the equations of motion in imaginary time. The resulting expression for Γ will be then particularized in the limit of $H \to H_c$, where H_c is the coercive field, and compared with the thermal transition probability rate (Γ_T) to get a measure of the critical temperature T_c between the quantum and thermal regimes [3].

A discussion about the experimental methodology that could demonstrate SQT is also included, in which the temperature dependence of the magnetic viscosity ($S(T)$) is measured with the objective is to observe a region in which S becomes independent of temperature, which would mean that the magnetic relaxation is mainly due to SQT driven transitions. This discussion is then focused on the results for maghemite single-domain NPs (γ-Fe_2O_3) [10].

II. MAGNETISM AT THE NANOSCALE

In this section, we present basic concepts for the description of the magnetic properties of particles with sizes in the nanoscale that are necessary for the calculations presented in Sec. IV. The basic equation governing the dynamics of the magnetization vector of a ferromagnetic material is the Landau and Lifshitz equation:

$$\frac{d\mathbf{M}}{dt} = -\gamma \mathbf{M} \times \frac{\delta E}{\delta \mathbf{M}} , \tag{1}$$

where $\gamma = \frac{ge}{2mc}$ is the gyromagnetic ratio and $\mathbf{M}$ the magnetization vector. It describes the precession of $\mathbf{M}$ around the effective field $\mathbf{H_{eff}} = \frac{\delta E}{\delta \mathbf{M}}$ than can be derived from the functional dependence of the magnet energy E on the magnetization. The different terms contributing to this energy will be described in the following subsections.

A. Magnetic Domains

Ferromagnetic (FM) materials tend to align their atomic spins in parallel to minimize the Heisenberg exchange, which is a strong short-ranged interaction of quantum mechanical origin. However, arising from the magnetic field they generate, the magnetostatic energy is increased. As a result, magnetic moments of ferromagnets will then arrange into regions of uniform magneti-

*e-mail address: faliagpu7@alumnes.ub.edu

zation, called magnetic domains, that point at different directions [7].

The size of domains is determined by the minimization of the total energy of the magnetic material, consisting on different competing terms such as magnetostatic, anisotropy and exchange energies. In this work, we will consider FM NPs in the single domain limit having a radius R below a critical size R_c, which typically ranges from few to 10ths of nanometers [7]. Therefore, they can be characterized by their total magnetic moment $\mathbf{M}$, consisting in the sum of the atomic moments of their magnetic ions.

B. Magnetic Anisotropy

The magnetization of a FM material tends to point along some preferential directions due to magnetic anisotropy energy. Anisotropy is mainly caused by the shape of the NP and the spin orbit coupling to the crystal lattice. In our work, we will focus on quasi spherical NP with an effective uniaxial anisotropy resulting from both contributions. In this case, the anisotropy energy can be represented as a polynomial series based on the angle (θ) that the magnetization ($\mathbf{M}$) forms with the principal crystallographic c-axis (see Fig. 1):

$$E_{mc}^{uniaxial} = K_0 + K_1 \sin^2\theta + ... \ , \tag{2}$$

where K_0 and K_1 are the 'anisotropy coefficients', constants that depend on the material properties and its temperature. The K_0 term is angular independent, and will be consequently ignored. For $K_1 > 0$ the easy-axis lies along the c-axis ($\theta = 0$).

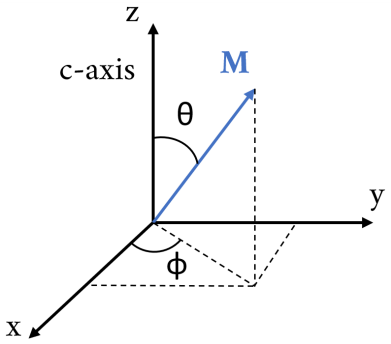

FIG. 1: Schematic representation of the magnetization in spherical coordinates.

C. Stoner-Wohlfarth model

The Stoner-Wohlfarth model is used to characterize the $\mathbf{M}$ rotation of a single domain NP in a magnetic field [8]. It assumes a rigid exchange coupling between the atomic spins of the NP and, as a result, the module of the total magnetic moment is constant. This means that our NP's atomic magnetic moments will all rotate as a single entity which is the total magnetization $\mathbf{M}$. When an external magnetic field $\mathbf{H}$ is applied to a FM NP, $\mathbf{M}$ will tend to point towards it in order to minimize the Zeeman energy (see Fig. 2). If the magnetic field is applied at an angle α from the easy axis, the total energy is given by:

$$E = K_u \sin^2\theta - MH\cos(\alpha - \theta) \ , \tag{3}$$

where the first term is due to the magnetic anisotropy (Eq. (2)) and the second one is the Zeeman energy.

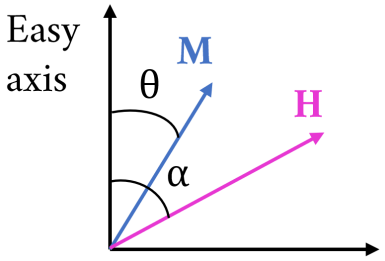

FIG. 2: Schematic representation of the magnetization direction change due to an external magnetic field.

III. PATH INTEGRAL METHOD

In classical mechanics, the trajectory that a particle follows from one point to another one is unique and will be the one that minimizes the classical action $\mathcal{S}$:

$$\mathcal{S} = \int_{t_0}^{t_f} \mathcal{L} dt \ , \tag{4}$$

where $\mathcal{L}$ is the Lagrangian of the system. In contrast, according to the path integral formulation of quantum mechanics [9], all possible trajectories must be taken into account when computing the transition amplitude between two states:

$$\langle x_f | \, e^{\frac{1}{\hbar}\hat{H}(t_f - t_0)} \, | x_0 \rangle = \int_{x_0}^{x_f} \mathcal{D}x e^{\frac{i}{\hbar}\mathcal{S}(t)} \ , \tag{5}$$

where $\mathcal{D}x$ indicates the sum over all possible paths between point x_0 and x_f, and the imaginary exponential function is the phase that represents the contribution of each path to the transition amplitude.

Switching to imaginary time with the substitution $\tau = it$, the exponential part of Eq. (5) becomes

$$B \equiv \frac{\mathcal{S}(\tau)}{\hbar} = -\frac{1}{\hbar}\int_{\tau_0}^{\tau_f} \mathcal{L}(\tau) d\tau \ . \tag{6}$$

Due to the similarity of Eq. (5) with the WKB probability transition rate, we can express it as

$$\Gamma = Ae^{-B} \ , \tag{7}$$

where A is a prefactor that accounts for fluctuations around the minimal action trajectory and has a value of the order of the frequency of small oscillations ω around $x = x_0$. For a macroscopic particle, the imaginary time action is large in comparison with $\hbar$, hence only trajectories near the one that minimizes the action will significantly contribute to the path integral. Consequently, we will approximate the latter using the saddle point approximation.

Particularizing this problem to a particle of mass m in a 1D potential $U(x)$ at $T \to 0$ [3]: $\mathcal{L}_\tau = \dot{x}_\tau^2/2 + U(x)$. The particle will tunnel from x_0 to x_f with an imaginary time period of $\tau_T = \hbar/T \to \infty$ and then the transition will take place from $\tau_0 = -\infty$ to $\tau_f = \infty$. The extremal trajectory that minimizes the action satisfies

$$\ddot{x} = \frac{dU(x)}{dx} \ , \tag{8}$$

which is the classical equation of motion for a particle in an inverted potential $-U(x)$ (see Fig. 3). There are three solutions to this equation that satisfy the condition of periodicity: $x = x_0$, $x = x_f$ and $x = x_b(\tau)$. The last one is the non-trivial solution called *bounce trajectory* or *instanton*. By switching to an imaginary time action, we

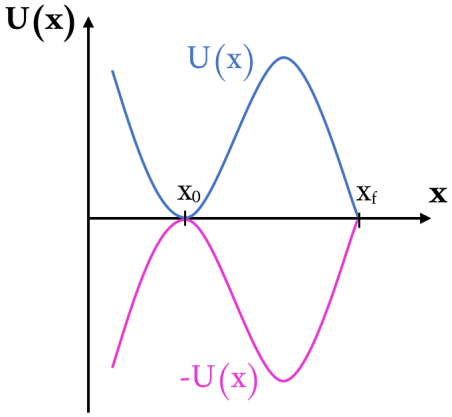

FIG. 3: Representation of the potential inversion when time is switched to an imaginary time.

have obtained a classical trajectory for a pseudoparticle (instanton) going down the slope of an inverted potential to tunnel though the barrier [11]. Summarizing, the exponential factor in the Γ corresponds to the Euclidean action evaluated along the instanton solution, which is the classical trajectory in the inverted potential $-U(x)$.

For the case of spin tunneling, all the above formalism can be adapted to the calculation of the SQT rate by changing the Lagrangian and the coordinates appearing in the path integral of Eq. (5). First, notice that now ϕ is the dynamic coordinate and, therefore, the conjugate momentum is $p = M_0/\gamma \cos\theta$. Using this correspondence, the action for spin tunneling becomes

$$\mathcal{S}(\tau) = \int_{-\infty}^{\infty} d\tau \left(-i\frac{M_0}{\gamma}\dot{\phi}\cos\theta - E(\theta,\phi) \right) \ , \tag{9}$$

where $E(\theta,\phi)$ is the total energy. Moreover, it is important to note that the equations of motion derived from this Lagrangian reproduce the Landau-Lifshitz Eq. (1), in imaginary time, correctly.

IV. TRANSITION RATE CALCULATION

The transition rate Γ will now be computed using the Stoner-Wohlfarth model and the integral path method for a particular case. It consists of a uniaxial single-domain NP with the easy-axis oriented in the 'c-axis', under the influence of an external magnetic field $\mathbf{H}$ applied perpendicular to it. Its potential energy per unit volume is [6]:

$$E(\theta,\phi) = K\sin^2\theta - HM_0\sin\theta\cos\phi + \frac{H^2M_0^2}{4K} \ , \tag{10}$$

where the third is a constant that enforces $E_{min} = 0$.

The two stable states ($E = 0$) for the magnetization are found at θ_0 and $\pi - \theta_0$, where: $\sin\theta_0 = 2KH/M_0$. Initially, $\mathbf{M_0}$ points at θ_0 and will tunnel to the other stable state (at $\pi - \theta_0$) overcoming the anisotropy energy barrier.

The external magnetic field is applied in order to reduce this barrier and increase the probability of MQT. At $H = H_c \equiv 2K/M_0$ (called coercive magnetic field), the barrier disappears and the two stable states merge into one stable state at $\theta = \pi/2$ (see Fig. 4).

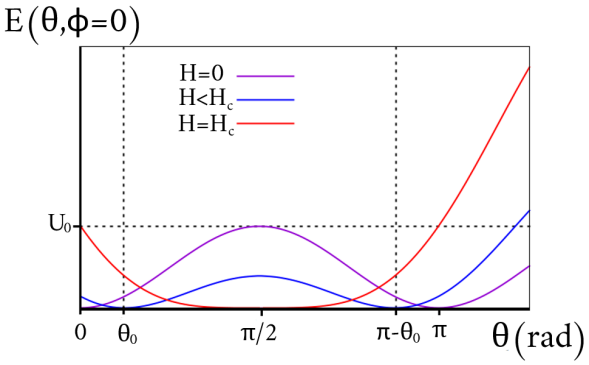

FIG. 4: Potential energy E per unit of volume as a function of θ at $\phi = 0$. Three different dependencies are shown for different values of the external magnetic field: $H = 0$ (violet), $H < H_c$ (blue) and $H = H_c$ (red).

To compute Γ at $T = 0$, the instanton solution will be calculated first. We begin by using the total energy expression Eq. (10) into the Landau-Lifshitz equation (1) expressed in the spherical coordinates of Fig. 1. After some algebra, we obtain the following two equations for the spherical angles:

$$\dot{\theta} = -iH\lambda\sin\phi \tag{11}$$

$$\dot{\phi} = i\frac{\gamma}{M_0}(2K\cos\theta - HM_0\cot\theta\cos\phi) \ , \tag{12}$$

where $\dot{\theta}$ and $\dot{\phi}$ are the derivatives of θ and ϕ with respect to the imaginary time τ.

Now, instead of solving the equations for $\theta(\tau), \phi(\tau)$ and substituting in Eq. (9), which leads to intricate calculations. We take advantage of energy conservation ($E = 0$), to obtain an expression that relates ϕ with θ, so that the two differential equations are reduced to just one:

$$\dot{\theta} = \frac{H\gamma}{2\sin\theta_0}\frac{\sin^2\theta - \sin^2\theta_0}{\sin\theta} \ . \tag{13}$$

The solution to this equation gives the instanton trajectory in spherical coordinates as

$$\cos\theta(\tau) = -\cos\theta_0 \tanh(\omega_b\tau) \tag{14}$$

$$\sin\phi(\tau) = i\frac{\cot^2\theta_0 \operatorname{sech}^2(\omega_b\tau)}{2\sqrt{1+\cot^2\theta_0 \operatorname{sech}^2(\omega_b\tau)}} \ , \tag{15}$$

where we have defined $\omega_b \equiv \frac{H\gamma}{2\tan\theta_0}$ that corresponds to half the frequency of small oscillations in either potential well.

The action for the particle can now be calculated using Eq. (9) and the instanton trajectory, along which the energy is conserved and, therefore, equal to zero:

$$\mathcal{S} = 2M_0\left(-\cos\theta_0 + \frac{1}{2}\ln\left(\frac{1+\cos\theta_0}{1-\cos\theta_0}\right)\right) \ . \tag{16}$$

Finally, the exact expression for the tunnel probability rate is then (using Eq. (7)):

$$\Gamma \propto \exp\left[-\frac{2M_0}{\hbar}\left(-\cos\theta_0 + \frac{1}{2}\ln\left(\frac{1+\cos\theta_0}{1-\cos\theta_0}\right)\right)\right] \tag{17}$$

(by saying 'exact' we refer to the exponential factor, the expression is not exact, it lacks the prefactor).

We would like to obtain now the dependence of Γ with H, which is the only parameter that can be tuned externally in this example. When $H \to H_c$, we expect Γ to be maximum as both the width and height of the energy barrier decrease when approaching the coercive field (see Fig. 4). To do so, we define $\epsilon \equiv 1 - H/H_c$ (closeness to the coercive field) and the (small) angle between the magnetic field and the magnetization vector $\delta = \frac{\pi}{2} - \theta$. Both tend to zero in this limit.

Therefore, the stable magnetization directions can be approximated by $\delta_0 = \pm\sqrt{2\epsilon}$. After performing a Taylor expansion of the cosine and the natural logarithm, the tunneling rate becomes:

$$\Gamma \propto \exp\left(-\frac{2M_0V}{3\hbar\gamma}(2\epsilon)^{3/2}\right) \ . \tag{18}$$

This expression confirms our premises. In order to observe SQT experimentally, a magnetic field perpendicular to the easy-axis with a value close to the coercive field (H_c) should be applied. The prefactor of Γ has not been calculated because the exponential component of the transition rate dominates (see [6] for details of the calculation).

V. ANALYSIS OF THE RESULTS

Thermal and Quantum regimes. SQT has been studied for a system at $T = 0$, yet in reality, finite temperature effects compete with the quantum ones. At finite T, thermal activation over an energy barrier U_0 can also occur, with a transition rate given by Arrhenius law [3]

$$\Gamma_T \propto \exp\left(-\frac{U_0}{k_BT}\right) \ . \tag{19}$$

Equating Γ_T to the T independent SQT rate found in Eq. (18), a critical temperature (T_c) below which dynamics will be governed by quantum effects can be obtained

$$T_c \approx \frac{3\hbar\gamma}{2k_B}\frac{U_0}{M_0}(2\epsilon)^{-3/2} \ . \tag{20}$$

Inserting typical K and M_0 values for a FM NP of 10 nm and using $\epsilon = 0.01$, T_c is be estimated to be in the range of $0.01 - 1$ K, depending on the material. Therefore, observation of SQT effects requires the study at very low temperatures.

Experimental manifestations of SQT. One way to evidence SQT, is through the study of the magnetic relaxation effect. It occurs when, after aligning $\mathbf{M}$ along an external field direction, it relaxes back to its equilibrium value once the magnetic field is suppressed

$$M(t) = M_0e^{-\Gamma t} \ , \tag{21}$$

where Γ will follow the Arrhenius law for $T > T_c$ Eq. (19) and the SQT temperature-independent rate expression for $T < T_c$ Eq. (17).

The Eq. (21) above assumes a magnetic NP with a single energy barrier. However, since in practice experiments are performed on a NP ensemble, there will be a distribution of volumes and anisotropy barriers. It is not difficult to show that when averaging the previous equation over a barrier distribution, the long time dependence of the total magnetization can be described by a logarithmic law as

$$M(t) = M_0(t_0)[1 - S(T,H)\ln(t/t_0)] \ , \tag{22}$$

where $S(T,H)$ is called magnetic viscosity, which is inversely proportional to the mean energy barrier. It should be linear with T if relaxation is driven by thermal fluctuations and should become constant at $T < T_c$, where SQT dominates.

In the 90's, several experiments to evidence this behaviour in NP were attempted [10]. As an example, we show in Fig. 5 the results for an assembly of maghemite NP with diameter < 10 nm. As can be seen in the inset, the viscosity seems to become independent on T below 2 K, although the results are not really conclusive due to the lack of points at lower temperatures. At the time, experiments with similar results were reported in NPs of other compositions and in thin films. Evidence of MQT

effects have been also reported in antiferromagnetic NPs [12] (where they should show up at higher T) and even in domain walls [4]. However, all of these experiments have been debated due the difficulties in the interpretation of the experimental techniques. Perhaps, the most clear-cut manifestation of MQT effects up to date has been reported in molecular magnets [5], which are small magnetic clusters, consisting of a small number of ions, with a total magnetic moment of the order of tenths of μ_B that can be chemically synthesized all equal. In this case, the steps that appear in the low T hysteresis loops are a manifestation of resonant QT between the discrete energy levels of the molecule.

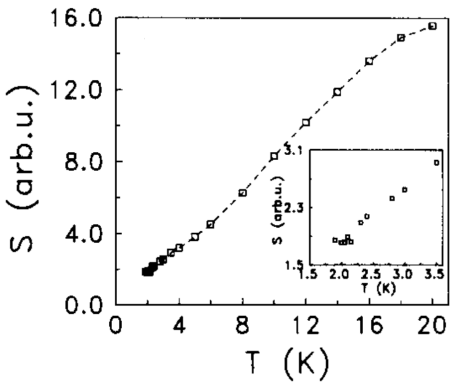

FIG. 5: Temperature dependence of the magnetic viscosity in arbitrary units measured in an assembly of maghemite NPs. The magnetic relaxation was recorded using a SQUID magnetometer after switching the field to $H = -50$ Oe. The inset shows a zoom of the lowest temperature region. (Reproduced from [10]).

VI. CONCLUSIONS

In this work, we have presented a general theoretical framework to compute tunneling rates in magnetic systems. Starting from the general path integral formulation to compute transition probabilities, we have shown how it can be adapted to the case of a tunneling variable that corresponds to the macroscopic magnetization of a single-domain ferromagnetic NP.

We have reviewed some key concepts of magnetism at the nanoscale relevant to the problem at hand, such as magnetic domains, magnetic anisotropy, and the Stoner-Wohlfath model for a macrospin at $T = 0$. From these, we have obtained an expression for the potential energy barrier of a single-domain NP, with uniaxial anisotropy, under the action of a transverse magnetic field along, as well as its energy, which are basic ingredients for the calculation of tunneling rates. We have used this exemplary case to show explicitly how to evaluate the tunneling exponent by using the instanton method. This approach have allowed us to obtain an exact analytic expression for the exponential factor of the tunneling rate.

Furthermore, we have analyzed the requirements for the most favorable experimental observation of SQT effects, calculating also the critical temperature below which quantum effects dominate over thermal effects. Our calculations reveal that by finely tuning the field to a value close to the coercive field and considering NP with sizes in the range of < 10 nm, SQT in a single NP could potentially be observed at temperatures lower than few K.

Lastly, we have reviewed some examples of experimental results that have attempted to demonstrate SQT, critically discussing the challenges and limitations encountered. While the theoretical basis for SQT is well-established, in our opinion, a conclusive experimental demonstration of this quantum effect in single NP is yet to be achieved. This is due to the difficulties in measuring the small magnetic moment associated to a single NP and the low temperatures required.

Acknowledgments

I would like to thank my advisor Òscar Iglesias for all the time that he has dedicated to help me understand some difficult concepts, and for all his kindness during the process.

I also thank my family and friends. All their support during these 4 years have been key to help me achieve the purpose of becoming a physics scientist.

[1] D. J. Griffiths, *Introduction to Quantum Mechanics* (Pearson Education, Inc. 2005, 2nd Ed.).
[2] E. M. Chudnovsky, Phys. Rev. Lett. **60**, 661 (1988).
[3] E. M. Chudnovsky and J. Tejada, *Macroscopic Quantum Tunneling of the Magnetic Moment* (Cambridge University Press, 1998).
[4] E. M. Chudnovsky, O. Iglesias and P. C. E. Stamp, Phys. Rev. B **46**, 5392 (1992).
[5] L. Thomas et al., Nature **383**, 145 (1996). J. R. Friedman et al., Phys. Rev. Lett. **76**, 3830 (1996).
[6] A. Garg and G.-H. Kim, Phys. Rev. B **45**, 12921 (1992).
[7] Kannan M. Krishnan, *Fundamentals and Applications of Magnetic Materials* (Cambridge University Press, 2016).
[8] E. C. Stoner and E. P. Wohlfarth, Phil. Trans. Royal Soc. London A **240**, 599 (1948).
[9] R. P. Feynman and A. R. Hibbs, *Quantum Mechanics and Path Integrals* (McGraw-Hill 1965).
[10] J. Tejada and X. Zhang, J. Magn. Magn. Mater. **140**, 1815 (1995).
[11] S. Coleman, *Aspects of symmetry* (Cambridge University Press, 1985).
[12] D.D. Awschalom et al., Phys. Rev. Lett., **68**, 3092 (1992).